PHYSICAL REVIEW B VOLUME 45, NUMBER 15 15 APRIL 1992-I

Thermal-stress-induced averaging of the Aharonov-Bohm oscillations in submicrometer Au loops

A. H. Verbruggen
Delft Institute of Microelectronics and Submicron Technology, Delft University of Technology, P.O. Box 5046, 2600 GA Delft, The Netherlands

H. Vloeberghs
Laboratorium voor Vaste Stof-Fysika en Magnetisme, Katholieke Universiteit Leuven, B-3001, Leuven, Belgium

P. A. M. Holweg
Delft Institute of Microelectronics and Submicron Technology, Delft University of Technology, P.O. Box 5046, 2600 GA Delft, The Netherlands

C. Van Haesendonck
Laboratorium voor Vaste Stof-Fysika en Magnetisme, Katholieke Universiteit Leuven, B-3001, Leuven, Belgium

S. Radelaar
Delft Institute of Microelectronics and Submicron Technology, Delft University of Technology, P.O. Box 5046, 2600 GA Delft, The Netherlands

Y. Bruynseraede
Laboratorium voor Vaste Stof-Fysika en Magnetisme, Katholieke Universiteit Leuven, B-3001, Leuven, Belgium
(Received 24 June 1991; revised manuscript received 13 January 1992)

We have prepared submicrometer-size loops of very high purity Au. At low fields, magnetoconductance oscillations with flux period h/e and $h/2e$ can be clearly observed. The sample-specific Aharonov-Bohm oscillations with flux period h/e are strongly modified by heating the Au loops up to $T=20$ K. These modifications probably result from the movement of dislocation line segments due to the thermal stress. The "annealing" at $T=20$ K allows us to simulate the stochastic impurity averaging of the h/e oscillations and to reconstruct the low-field $h/2e$ oscillations caused by the coherent backscattering around the loop. This $h/2e$ signal is described very well by the weak electron localization theory, which takes into account the detailed geometry of the voltage and current probes.

The magnetoconductance of mesoscopic samples (i.e., samples with a size smaller than the phase coherence length L_ϕ) shows fluctuations, which are characteristic of the specific distribution of the elastic scattering centers within the sample.[1,2] The amplitude of these magneto-fingerprints,[2] which depends on temperature and actual sample geometry, is of the order of e^2/h. The rather large fluctuation amplitude often prevents the (accurate) observation of other phenomena occurring simultaneously in the mesoscopic structures. The influence of the magnetoconductance fluctuations can be suppressed by relying on their stochastic "self-averaging" in larger samples consisting of many independent mesoscopic units.[3,4] As an example we mention the observation of one-dimensional subband effects in narrow metal-oxide-semiconductor field-effect-transitor structures by measuring a large number of quantum wires in parallel.[5] For a "single" mesoscopic structure, stochastic averaging of the conductance fluctuations can be achieved by repeatedly heating the sample to room temperature or by repeatedly applying a short electrical pulse and averaging the magnetofingerprints measured after every heating cycle or pulse.[6] The success of this rather violent approach is limited because most mesoscopic structures are very fragile. In this paper we will show that carefully "annealing" a mesoscopic Au sample at 20 K is already sufficient to produce uncorrelated fluctuation patterns at $T=1.3$ K. This allows us to simulate the stochastic impurity averaging of the fluctuations. The configuration of the elastic scattering centers is probably altered by the movement of dislocation line segments.

The sample-specific fluctuations of the magnetoconductance result from the direct interference between splitted electron waves, which is tuned by the applied magnetic field via the Aharonov-Bohm[7] (AB) effect. For a loop geometry, the electron waves traveling along both arms of the loop enclose a well-defined area and the interference effects become observable as magnetoconductance oscillations with a flux period $\Phi_0=h/e$.[8] As predicted by Altshuler, Aronov, and Spivak (AAS),[9] the interference between electron waves, which travel completely around a loop along time-reversed paths, causes oscillations with flux period $\Phi_0/2=h/2e$. The AAS $h/2e$ oscillations survive the ensemble averaging in large arrays of loops.[10,11] Both the AAS $h/2e$ oscillations and the weak electron localization (WEL) effects in thin metal films result from the coherent backscattering and can only be observed at low magnetic fields.[9]

The magnetoconductance oscillations are damped exponentially when the phase coherence length L_ϕ is reduced

by the spin-flip scattering at residual magnetic impurities. Experimentally[3,12] the AAS $h/2e$ oscillations only appear when L_ϕ becomes comparable to the loop circumference, requiring a magnetic contamination of the order of 1 ppm or smaller. The AB h/e oscillations turn out to be less sensitive to the magnetic scattering, since the phase coherence may be restricted to half the loop circumference. Moreover, the h/e oscillations survive in a high magnetic field, where the spin-flip scattering is inhibited by the Zeeman splitting of the energy levels.[13]

We have prepared submicrometer Au loops with a very low magnetic impurity content. The phase coherence length L_ϕ is sufficiently long to allow a clear observation at low magnetic fields of both the AAS $h/2e$ oscillations and the AB h/e oscillations. When the Au loops are annealed at $T=20$ K, both the phase and the amplitude of the sample-specific AB h/e oscillations, which are asymmetric about zero field,[14] are modified. By properly averaging the magnetoconductance traces obtained after each annealing cycle, the pure AAS $h/2e$ oscillations, which are symmetric about zero field, can be reconstructed. This allows us to check in detail the influence of the voltage and current probes[15] on the coherent backscattering around the mesoscopic loop. A similar influence of the sample geometry has been reported for large arrays of loops.[11,16]

The submicrometer Au loops are obtained by combining electron-beam lithography and lift-off techniques. A Philips electron beam pattern generator EBPG/3 is used for writing the contact pads, while the fine line pattern is delineated by a Philips PSEM500 scanning electron microscope equipped with a homemade pattern generator. A favorable lift-off undercut profile is obtained with a PMMA bilayer resist (100-nm du Pont Elvacite 2041 on top of 100-nm du Pont Elvacite 2010).

The substrate is a Si wafer covered with 60-nm low-pressure chemical vapor deposition silicon nitride. Thermal evaporation of very high purity gold (99.9999%) is used to obtain the Au fine lines (thickness $t=35$ nm). In order to obtain a smooth film surface, without any cracks appearing at the grain boundaries, the evaporation is done in a reduced helium atmosphere ($p\simeq 10^{-4}$ Torr). The film smoothness on a submicrometer scale has been confirmed by STM topography in air. Although our preparation technique allowed the fabrication of many high-quality loop structures, we will restrict our presentation to the results obtained for one typical Au loop. An electron micrograph for this Au loop is shown in the inset in Fig. 1. From the micrograph we find that this loop has a radius $r\simeq 350$ nm and a linewidth $w\simeq$ 35 nm. At $T=1.3$ K the loop resistance $R=20.2$ Ω, corresponding to a conductance $G=1280$ in units of e^2/h.

At high magnetic fields ($1<B<4$ T), the Au loop shows pronounced h/e oscillations and a much weaker harmonic $h/2e$ signal. The beating conductance oscillations, with rms amplitude $\Delta G\simeq 0.1e^2/h$ at $T=1.3$ K, are superimposed upon a slowly varying background, in agreement with previous experiments.[8] From the width of the autocorrelation function for the aperiodic fluctuations[17] we calculate a phase coherence length $L_\phi(T=1.3\ \text{K})=2.3\pm 0.4$ μm. Although L_ϕ exceeds half the loop circumference $\pi r\simeq 1.1$ μm, i.e., negligible exponential damping of the AB oscillations occurs, the h/e rms oscillation amplitude is reduced considerably by thermal averaging.[2] We estimate that for our Au loop $\Delta G(T\rightarrow 0)\simeq 0.5e^2/h$.

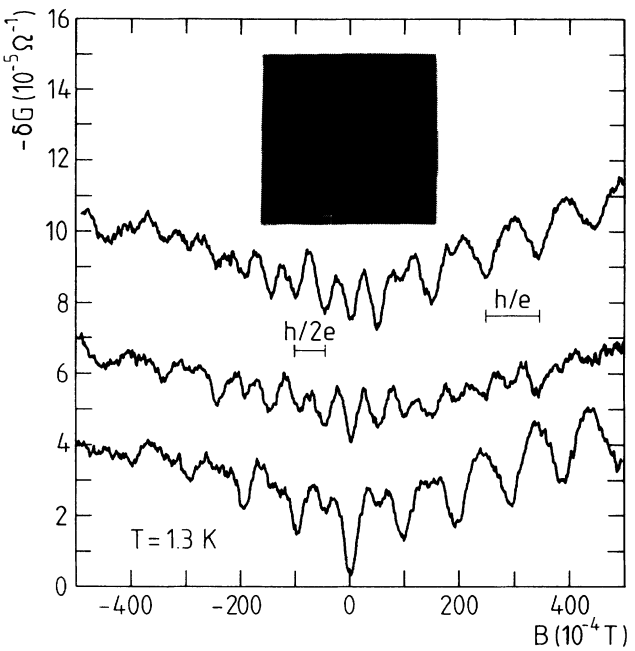

FIG. 1. Typical low-field magnetoconductance traces for a mesoscopic Au loop. After recording each of the traces, the loop is heated up to $T=20$ K and cooled down again to $T=1.3$ K. The inset shows an electron micrograph of the mesoscopic Au loop. The marker corresponds to 1 μm.

Figure 1 shows three typical magnetoconductance traces near zero field at $T=1.3$ K. Oscillations with flux period h/e and $h/2e$ are clearly observable, indicating that both direct interference and coherent backscattering are present. After recording each of the traces, the Au loop is heated up to $T=20$ K and cooled again to $T=1.3$ K. We see that after each of the annealing cycles another magnetofingerprint is obtained. This is interpreted as evidence for a transition towards another configuration of the elastic scattering centers within the sample. A simple thermally induced motion of the scattering centers can be excluded; at our low annealing temperature thermally activated motion of impurities and defects, which generally have activation energies for migration of more than 100 meV, is no longer possible. The presence of "two-level systems" in the disordered Au metal can also give rise to a change of the scattering potential.[18] The very low noise level ($0.4<T<30$ K) in our Au loops, however, points to a minor influence of the two-level systems on the magnetofingerprints.[19]

We believe that the changes of the magnetoconductance traces in Fig. 1 are directly related to the fact that the thermal expansion of the gold wires and the underlying Si_3N_4 substrate differs by an order of magnitude. This causes a considerable, temperature-dependent stress in the Au films, which decreases with increasing temperature.

The modified configuration of the scattering centers in our Au loop probably results from a movement of dislocation segments, mainly through the movement of dislocation kinks.[20] When the shear stress on the glide planes changes as a function of temperature, dislocation segments, which do not run parallel to one of the close-packed directions, will move sideways by the displacement of kinks. Since the purity of our Au samples is very high, pinning of the dislocations will be governed by dislocation intersection and grain boundaries. For the annealing at $T=20$ K, the influence of the movement of the dislocations on the average conductance process is small: The loop conductance at $T=1.3$ K remains constant within e^2/h, even after more than 20 annealing treatments.

Using digital filtering it is possible to separate the h/e from the $h/2e$ oscillations in the low-field magnetoconductance trace. When only the spectral information around the h/e peak in the Fourier spectrum is retained (bandpass filtering), we can isolate the influence of the direct interference effects. Typical interference patterns are shown by the three lower traces in Fig. 2. The h/e magnetoconductance traces are obviously not symmetric about zero field. The solid curves represent a phase-shifted cosine function. The observed phase shifts at zero field vary randomly between $-\pi$ and π. Due to the magnetic flux penetrating the arms of the loop, the amplitude as well as the phase shift are slowly varying and random functions of the magnetic field, explaining the small deviations between the solid curves and the data points in Fig. 2. Previous work[14] indicated that the asymmetry of the magnetoconductance fluctuations in mesoscopic samples is caused by the four-terminal measuring technique. This technique implies that, on a mesoscopic scale, the off-diagonal Onsager coefficients will influence not only the Hall conductance but also the longitudinal conductance. Consequently, the symmetry relation $G(B)=G(-B)$ no longer holds for a mesoscopic four-terminal measurement.

The presence of the random phase shifts will cause the destruction of the h/e effects in large arrays of loops. The top trace shown in Fig. 2 has been obtained by averaging the filtered h/e oscillations of 25 different low-field magnetoconductance traces. As expected for stochastic averaging of incoherent signals, the h/e oscillation amplitude shows a $N^{-1/2}$ dependence, with N the number of annealing cycles used for the averaging procedure. A similar stochastic impurity averaging of the AB h/e oscillations has been demonstrated for finite arrays of Ag loops in series.[3] In the latter experiment a self-averaging of the h/e oscillations occurred, since the loops with a size comparable to L_ϕ behaved as independent mesoscopic units. It is important to note that the stochastic impurity averaging occurs independently of the thermal averaging,[2] which reduces our h/e oscillation amplitude by a factor of 5 at $T=1.3$ K.

In contrast to the AB h/e oscillations shown in Fig. 2, the magnetoconductance induced by the coherent backscattering does not depend upon the specific defect configuration and is perfectly symmetric about zero field. In Fig. 3, the triangular symbols represent the symmetric part of the low-field magnetoconductance, which survives after averaging 25 different traces. The AAS $h/2e$ oscillations are superimposed upon the slowly varying WEL background caused by the magnetic flux piercing the arms of the loop.[9] The residual h/e signal (see top trace in Fig. 2) has been removed by digital filtering (notch filter).

The WEL background as well as the AAS $h/2e$ oscillations can be described by the theoretical calculations[15] that take into account the influence of the voltage and current probes. Due to the disorder present in these probes, the interference effects, which extend over a distance of the order of L_ϕ, will depend on the details of the four-terminal geometry shown in the inset in Fig. 1. The solid curve in Fig. 3 represents the result of the theoretical calculation. The loop radius $r=365$ nm and the linewidth $w=30$ nm obtained from this calculation agree with the

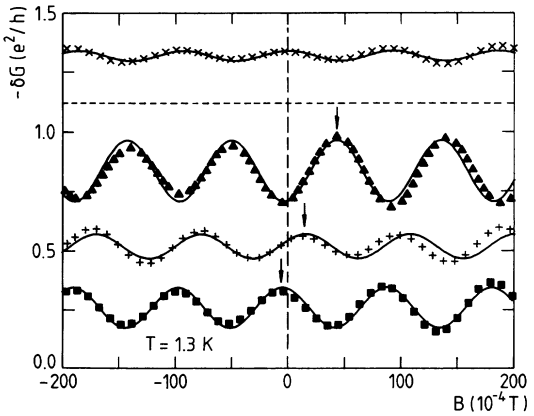

FIG. 2. Aharonov-Bohm h/e oscillations near zero field. The lower three traces are obtained by digital bandpass filtering of magnetoconductance traces similar to the ones shown in Fig. 1. The upper trace is obtained by averaging 25 filtered traces. The solid curves correspond to a phase-shifted cosine function.

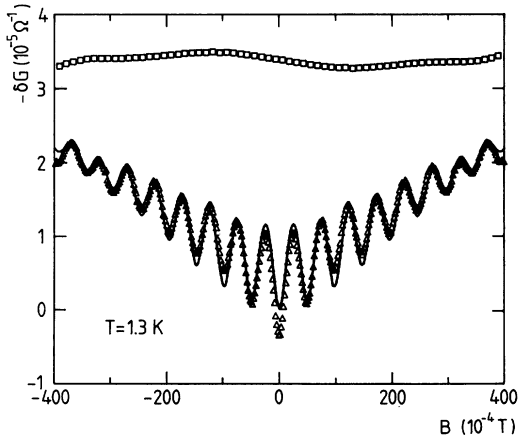

FIG. 3. Symmetric part of the low-field magnetoconductance obtained by the averaging of 25 traces and after removal of the Aharonov-Bohm h/e oscillations by digital filtering (triangles). The $h/2e$ oscillations can be described by the weak electron localization theory (solid curve) taking into account the detailed probe geometry [15]. The squares correspond to the antisymmetric part of the aperiodic background.

micrograph in the inset in Fig. 1. The deviation between theory and experiment near zero field is probably caused by the symmetric part of the aperiodic fluctuations, which could not be removed completely by the averaging procedure. The deviation is indeed comparable to the amplitude of the averaged antisymmetric part of the aperiodic background, which is represented by the square symbols in Fig. 3. The periodic oscillations have been removed by digital filtering.

From our comparison with the WEL theory we obtain a phase coherence length $L_\phi \simeq 1.4 \pm 0.2$ μm, which should be compared to the value $L_\phi \simeq 2.3 \pm 0.4$ μm obtained from the high-field AB fluctuations.[17] The different L_ϕ values can be accounted for by the magnetic-field dependence[13] of the dephasing by spin-flip scattering[21] at residual magnetic impurities ($\sim$0.1 ppm). The WEL magnetoconductance, which has been measured for two-dimensional Au films evaporated simultaneously with the Au loops, reveals a low-field phase coherence length $L_\phi \simeq 4.0$ μm. This indicates that an important reduction of the phase coherence occurs because of the quasi-one-dimensional line structure,[22] as confirmed by our measurements of the WEL effects for very long Au lines.

In conclusion, we have shown that the low-field magnetoconductance of very high purity, mesoscopic Au loops is strongly modified by annealing the loops at $T=20$ K. We believe that these modifications result from a change in the defect configuration caused by the movement of dislocation segments. By averaging the magnetoconductance obtained after different annealing cycles, we are able to simulate the stochastic impurity averaging of the h/e oscillations. The $h/2e$ oscillations largely survive the averaging process and can be nicely described by the theory for the weak electron localization, provided the detailed probe geometry is taken into account.

The authors are much indebted to V. Chandrasekhar, P. Santhanam, C. Umbach, R. B. Laibowitz, and R. Webb for very helpful discussions. The research at the Katholieke Universiteit Leuven has been supported by the Belgian Inter-University Institute for Nuclear Sciences (IIKW), the Inter-University Attraction Poles (IUAP), and Concerted Action (GOA) programs, as well as by the Research Council of the Katholieke Universiteit Leuven. H.V. and C.V.H. have also benefited from the financial support of the Belgian National Fund for Scientific Research (NFWO). The Delft Institute of Microelectronics and Submicron Technology is supported by the Stichting voor Fundamenteel Onderzoek der Materie (FOM).

[1] B. L. Altshuler, Pis'ma Zh. Eksp. Teor. Fiz. **41**, 530 (1985) [JETP Lett. **41**, 648 (1985)]; B. L. Altshuler and B. Z. Spivak, *ibid.* **42**, 363 (1985) [*ibid.* **42**, 447 (1986)].

[2] P. A. Lee and A. D. Stone, Phys. Rev. Lett. **55**, 1622 (1985); P. A. Lee, A. D. Stone, and H. Fukuyama, Phys. Rev. B **35**, 1039 (1987).

[3] C. P. Umbach, C. Van Haesendonck, R. B. Laibowitz, S. Washburn, and R. A. Webb, Phys. Rev. Lett. **56**, 386 (1986).

[4] A. Benoit, C. P. Umbach, R. B. Laibowitz, and R. A. Webb, Phys. Rev. Lett. **58**, 2343 (1987).

[5] J. R. Gao *et al.*, Phys. Rev. B **41**, 12315 (1990).

[6] D. Mailly and D. Sanquer, in *Quantum Coherence in Mesoscopic Systems,* edited by B. Kramer (Plenum, New York, 1991), p. 401.

[7] Y. Aharonov and D. Bohm, Phys. Rev. **115**, 485 (1959).

[8] R. A. Webb, S. Washburn, C. P. Umbach, and R. B. Laibowitz, Phys. Rev. Lett. **54**, 2696 (1985).

[9] B. L. Altshuler, A. G. Aronov, and B. Z. Spivak, Pis'ma Zh. Eksp. Teor. Fiz. **33**, 101 (1981) [JETP Lett. **33**, 94 (1981)].

[10] B. Pannetier, J. Chaussy, R. Rammal, and P. Gandit, Phys. Rev. Lett. **53**, 718 (1984).

[11] G. J. Dolan, J. C. Licini, and D. J. Bishop, Phys. Rev. Lett. **56**, 1493 (1986).

[12] V. Chandrasekhar, M. J. Rooks, S. Wind, and D. E. Prober, Phys. Rev. Lett. **55**, 1610 (1985).

[13] A. Benoit *et al.*, in *Anderson Localization,* edited by T. Ando and H. Fukuyama (Springer-Verlag, Berlin, 1988), p. 346.

[14] M. Büttiker, Phys. Rev. Lett. **57**, 1761 (1986); A. D. Benoit, S. Washburn, C. P. Umbach, R. B. Laibowitz, and R. A. Webb, *ibid.* **57**, 1765 (1986).

[15] P. Santhanam, Phys. Rev. B **39**, 2541 (1989); V. Chandrasekhar, P. Santhanam, and D. E. Prober, *ibid.* **44**, 11203 (1991).

[16] B. Douçot and R. Rammal, Phys. Rev. Lett. **55**, 1148 (1985).

[17] C. W. J. Beenakker and H. van Houten, Phys. Rev. B **37**, 6544 (1988).

[18] K. S. Ralls and R. A. Buhrman, Phys. Rev. Lett. **60**, 2434 (1988); N. M. Zimmermann, B. Golding, and W. H. Haemmerle, *ibid.* **67**, 1322 (1991).

[19] N. O. Birge, B. Golding, and W. H. Haemmerle, Phys. Rev. Lett. **62**, 195 (1989).

[20] F. R. N. Nabarro, *Theory of Crystal Dislocations* (Oxford Univ. Press, London, 1967).

[21] V. Chandrasekhar, P. Santhanam, and D. E. Prober, Phys. Rev. B **42**, 6823 (1990).

[22] S. Wind, M. J. Rooks, V. Chandrasekhar, and D. E. Prober, Phys. Rev. Lett. **57**, 633 (1986).

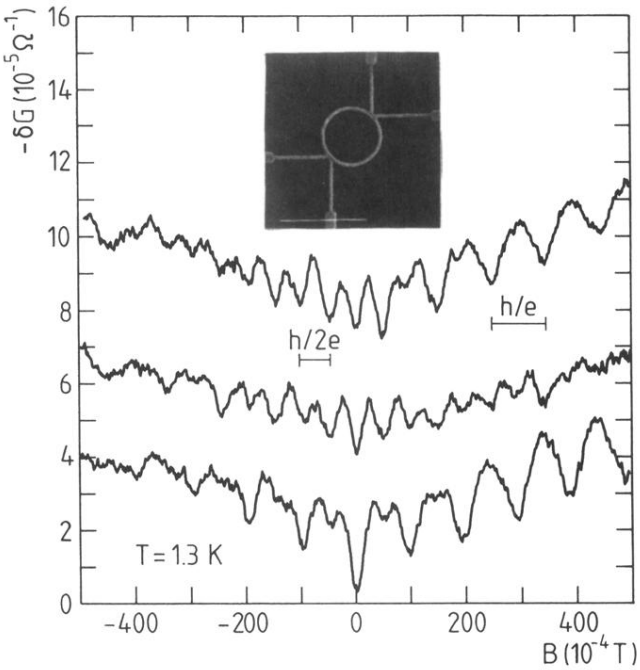

FIG. 1. Typical low-field magnetoconductance traces for a mesoscopic Au loop. After recording each of the traces, the loop is heated up to $T=20$ K and cooled down again to $T=1.3$ K. The inset shows an electron micrograph of the mesoscopic Au loop. The marker corresponds to 1 μm.